Characteristic regions on the energy landscape of MgF_2

2001 J. Phys. A: Math. Gen. 34 4041

(http://iopscience.iop.org/0305-4470/34/19/306)

INSTITUTE OF PHYSICS PUBLISHING JOURNAL OF PHYSICS A: MATHEMATICAL AND GENERAL

J. Phys. A: Math. Gen. **34** (2001) 4041–4052 www.iop.org/Journals/ja PII: S0305-4470(01)19358-3

Characteristic regions on the energy landscape of MgF_2

M A C Wevers, J C Schön and M Jansen

Max-Planck-Institut für Festkörperforschung, Heisenbergstrasse 1, D-70569 Stuttgart, Germany

Received 20 November 2000, in final form 2 March 2001

Abstract

High-dimensional energy landscapes of complex systems often exhibit a very complicated structure, with many local minima separated by a multitude of barriers of various heights. For the analysis of the dynamics on such landscapes, simplified models based on combining many microstates to form physically relevant macrostates are of great advantage. In particular, knowledge of the relative sizes of minimum and transition regions is crucial. As an example, we analyse transitions in low-energy regions belonging to a simple model of the crystalline compound MgF_2. We find that the minimum regions, i.e. the states associated with only one particular minimum, extend to energies far above the saddle points, and we show that the size of the transition regions is small compared with the minimum regions.

PACS numbers: 0250, 0270L, 0590, 8820K

1. Introduction

Knowledge of the structure and properties of energy hypersurfaces is important for understanding the dynamic and static features of a large variety of complex physical and chemical systems [1–3]. Examples range from the relaxation dynamics in glasses [4–8] and spin glasses [9, 10], over the folding transformation in proteins [11–14] and the study of the properties of clusters [15], polymers [16] and solids [17, 18], to the efficiency of combinatorial optimization algorithms [19, 20]. Thus, a number of methods have been developed to determine some of the global and local features of energy landscapes [21–28], for example local minima and the barriers between them. These results have been used to construct highly simplified representations of the energy landscape such as single-lump tree graphs [29,30] (also called, for example, disconnection trees [31], disconnectivity graphs [16] or one-dimensional projections [32]), where basins around local minima of the energy landscape are represented as nodes of a tree graph.

In previous work [33], we have shown how the threshold algorithm [30, 34] can be used to go beyond the purely energetic aspects of the barriers in the landscape by constructing the so-called transition maps [33], in addition to the tree graphs. Together, they show the observed connections and transition probabilities among the local minima, and include for

0305-4470/01/194041+12$30.00

each minimum the so-called return energies $E^{\mathrm{R}}_{100\%}$ and $E^{\mathrm{R}}_{80\%}$ (previously also called return probabilities), which are a measure of the difficulty of leaving a minimum region. The energy landscapes of simplified models of MgF_2 and CaF_2 [35] served as example systems.

In this paper, we extend our analysis of the barrier structure of energy landscapes by addressing the question of how regions of the energy landscape that energetically lie above the barrier among the minima can be classified. For this, we are going to perform both global explorations of pockets of the landscape containing several minima and a more detailed analysis of several transitions between low-lying minima in the system MgF_2. Together with the transition maps and the tree graphs, this information can serve as input for simplified representations of landscapes that can be used to model the dynamics of such systems.

2. Model system and method

2.1. Model

The global analysis of the energy landscape of a solid is highly non-trivial, and even nowadays it is necessary to employ a number of radical simplifications to achieve this task. Since the simplified model of MgF_2 that we have used for our investigations has already been presented in detail in earlier papers [33, 35], we restrict ourselves to a short summary and refer to that work for details regarding the geometric structures of the local minima found during the global optimization.

In the model, we have introduced periodic boundary conditions, and we employ two formula units ($z = 2$) of atoms per simulation cell. Furthermore, we use a simple empirical two-body interaction potential between the atoms consisting of a Coulomb and a Lennard-Jones term, in order to allow for fast calculations of the energy of a given configuration [35]. Over 50 structurally different local minima have been found, with the global minimum (VI-a in figure 1) corresponding to the experimentally observed rutile structure. Figure 1 shows the simplified (only the seven most prominent basins are depicted) tree graph of the system, for reference. The paper presented here focuses on the low-energy region containing the major minima VI-a and VII-a[1].

2.2. Algorithms

For the investigation of the transitions among the minima, several algorithms were used that explore the landscape or well defined sub-regions thereof stochastically via random walks according to a prescribed move class. In all instances, the move class consisted of random movements of single atoms (85%) and variations of the cell parameters (15%). For the Monte Carlo algorithm, the Metropolis acceptance criterion was employed with a constant temperature parameter T [36]. For $T = 0$, only moves are accepted that do not raise the energy. This corresponds to the second algorithm employed, the (stochastic) quench algorithm. Finally, the so-called threshold algorithm [30] proceeds as follows: starting from a local minimum m_0, the system explores the landscape for n_{thr} random steps, where every move is accepted that does not cross a prescribed energy lid L_k (threshold phase). During this random walk, quench runs (of length n_{qu}) ending in minima m_A are performed periodically every n_{h} steps starting from halting points $x_i^{(h)}$ numbered with i (quench phase). If $m_A \neq m_0$, a transition has taken place at a lid value of L_k. In general, this threshold–quench combination is repeated for a sequence of consecutive lid values, and the whole procedure is applied to all local minima of

[1] Several minor local minima observed in the course of this investigation but not listed in earlier work [35] are given in table 1.

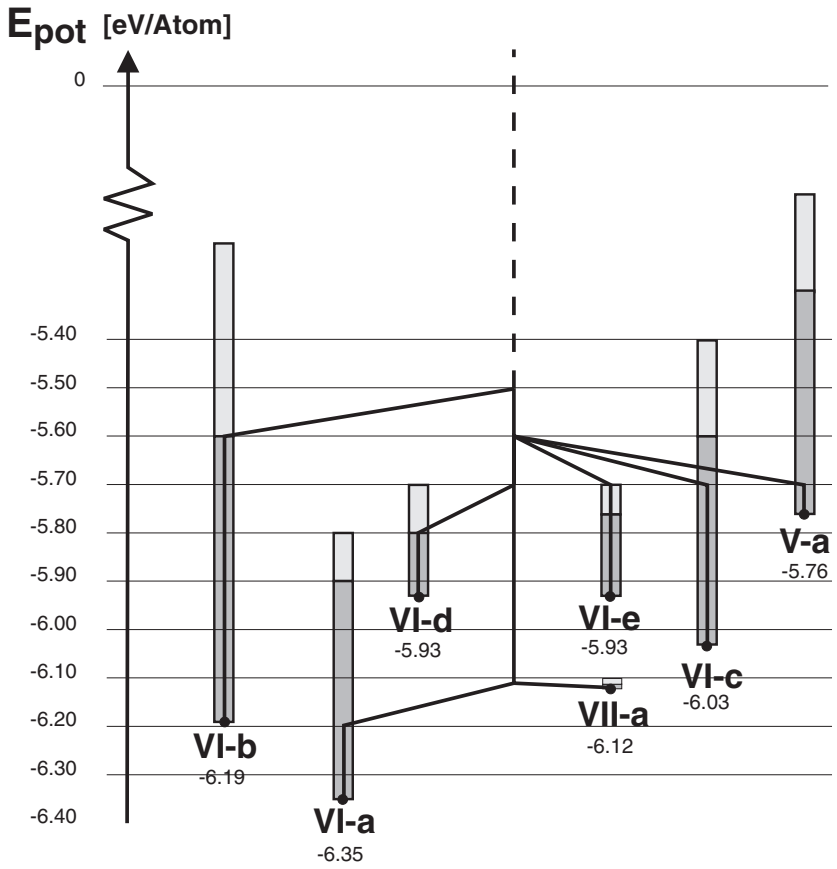

Figure 1. Tree-graph diagram representation of the energy landscape of MgF_2 showing the most important minimum regions (cf [33, 35]). The nodes at the ends of the branches represent local minima and are located at the energies of these minima: VI-a—rutile, VI-b—the anatase type, VI-c—a half-filled NaCl variant, VI-d—the $CdCl_2$ type, and VI-e, VII-a and V-a—three structures with prismatic, sevenfold and fivefold coordination of Mg by F, respectively. The intersection of an edge emanating from a minimum with the remainder of the graph indicates that a transition between this minimum and some other minima is possible without exceeding the energy at which the vertex is located. By construction, this graph representation contains no loops, resulting in a tree graph. The heights of the bars at the minima indicate the so-called return energies $E^{\mathrm{R}}_{100\%}$ (dark) and $E^{\mathrm{R}}_{80\%}$ (light), respectively [33].

interest. The sampled part of the configuration space up to L_k starting from m_0 is called a pocket $\mathcal{P}(L_k; m_0)$.

These threshold runs are repeated many times, and, in addition, the quench runs at each point $x_i^{(h)}$ are repeated for several random numbers. Based on a series of test runs (cf the appendix), we have chosen $n_{\mathrm{thr}} = 2.5 \times 10^5$ as a standard length for threshold runs.

2.3. Characteristic regions

If the energy of the lid is higher than a neighbouring barrier, several local minima are, in principle, accessible by a quench run from a halting point $x^{(h)}$ above such a barrier. The probability of reaching one of the accessible local minima m_A in a stochastic quench run from

Table 1. Crystallographic data for the new (idealized) local minima.

Minimum E (eV/atom)	Space group (crystal system)	Cell constants a, b, c (Å); α, β, γ	Atom	x	y	z
V-b[a]	P $4/nmm$ (129),	$a = 3.623, c = 4.766$	F2 (2c)	1/4	3/4	1/2
−5.886	tetragonal	$\alpha = 90.00, \beta = 90.00, \gamma = 90.00$	F1 (2a)	1/4	1/4	0.904
			Mg (2a)	1/4	1/4	0.306
V-c[b]	P $mn2_1$ (31),	$a = 3.799, b = 3.726, c = 4.800$	F2 (2a)	1/2	0.389	0.118
−5.920	orthorhombic	$\alpha = 90.00, \beta = 90.00, \gamma = 90.00$	F1 (2a)	1/2	0.572	0.734
			Mg (2a)	1/2	0.899	0.246
VI-g[c]	C mma (67),	$a = 5.194, b = 5.286, c = 4.743$	Mg (4g)	1/2	3/4	0.301
−5.999	orthorhombic	$\alpha = 90.00, \beta = 90.00, \gamma = 90.00$	F2 (4f)	1/4	1/2	1/2
			F1 (4e)	1/4	3/4	0
VII-d[d]	P $2_1/m$ (11),	$a = 3.586, b = 3.428, c = 5.243$	Mg (2e)	0.690	3/4	0.760
−6.085	monoclinic	$\alpha = 90.00, \beta = 100.74, \gamma = 90.00$	F2 (2e)	0.766	1/4	0.081
			F1 (2e)	0.250	3/4	0.414

[a] CN = 5, stacked sheets of chess-board-like alternating tetragonal pyramids.
[b] CN = 5, network of (distorted) corner-connected pyramids with central atom shifted from centre, cations build pyramids around anions too.
[c] CN = 6, prisms, 1/2 NiAs with a plane of prisms shifted by 1/2, hcp of anions.
[d] CN = 7, distorted VII-a structure with one twisted edge of the mono-capped prisms.

a given starting configuration $x^{(h)}$ is denoted $P(A; x^{(h)})$. The set of these probabilities as a function of $x^{(h)}$, $W(x^{(h)}) = \{P(A; x^{(h)})\}$ ($\sum_A P(A; x^{(h)}) = 1$) yields important information about the effective connectivity of the landscape at energies above the first saddle points. Using a suitable binning procedure, one can group all states with similar W together in characteristic regions[2] $\mathcal{C}$. States that are associated with more than one minimum region form the transition (saddle) regions of the landscape.

For practical purposes, we have chosen a very simple and rather rough criterion for classifying the configurations encountered: all states from which 80% or more of the quench runs reach one specific local minimum m_A are assigned to its minimum region or its boundary $\mathcal{C}_{P(A)\geqslant 0.8}$. The remaining states are associated with various transition regions between particular minima, e.g. $\mathcal{C}_{0.4\leqslant P(A)\leqslant 0.6 \wedge 0.4\leqslant P(B)\leqslant 0.6}$.

These characteristic regions can serve as building blocks for a graphlike representation of the landscape, which takes the relative sizes of the minimum and transition regions, and their connectivity, into account. In certain instances, this structure can be mapped onto a tree model, but in general the landscape will be represented as a graph containing circuits[3].

Ideally, the characteristic regions would be locally ergodic [18], i.e. the time to leave such a region would be much longer than the local equilibration time, $\tau_{\mathrm{esc}} \gg \tau_{\mathrm{eq}}$. If that is the case, one can analyse the relaxation and time evolution of the system on the landscape using a separation of timescales. For $t < \tau_{\mathrm{eq}}$ one studies the dynamics within one (isolated) characteristic region, while for $t > \tau_{\mathrm{esc}}$ one only needs to deal with the (stochastic) dynamics on the graph [29, 38–40].

[2] If the characteristic regions consisted of disconnected pieces, one would usually split them up accordingly.
[3] Such graphs have also been observed as a result of coarse-graining procedures that identify regions without internal energetic barriers on discrete landscapes [37, 38].

2.4. Representation using characteristic coordinates

Sometimes it is possible to give a highly simplified visual representation of the probability of entering a certain minimum, if relevant static and/or dynamic aspects of a pocket can be captured by a (few) characteristic coordinate(s) Q. All the other 'dimensions' of the landscape are suppressed, and the saddle point in such a one- (low-) dimensional representation corresponds to the lowest saddle between the two minima. For each value of Q, we plot the probabilities $P(A)$ and $P(B)$ to reach minimum m_A or m_B, respectively, 'averaged' over all configurations x_Q within the pocket with the same value of Q.

One should note that this simplified representation is most meaningful if for a given value of Q (and energy E) $W(x_Q)$ does not vary much as function of x_Q. In such a case, the union of the points x_Q (with similar $W(x_Q)$) would constitute a characteristic region[4], as defined in section 2.3, and one would be justified in replacing the individual distributions $P(A; x_Q)$ by their 'average' $P(A; Q)$ for each value of Q.

3. Results

3.1. Global explorations

As a first step, we studied the statistical distribution of the outcomes of different quench runs departing from the same halting point $x_i^{(h)}$, for a number of halting points essentially randomly distributed within the pockets under investigation. As starting points for the quench runs, we selected the endpoints of the last threshold phase for standard ($n_{\mathrm{thr}} = 2.5 \times 10^5$) and very long runs ($n_{\mathrm{thr}} = 5 \times 10^5$), performing ten different quenches for the lid values $L_k = -5.9, -5.7, -5.6, -5.5, -5.4$ eV/atom, and 20 for $L_k = -5.8$ eV/atom, respectively. In addition several intermediate halting points for $L_k = -5.6, -5.4, -5.0$ eV/atom were chosen as starting points. Each quench run consisted of up to 5×10^4 steps. We observed that the distribution of local minima found when starting from the end points of standard and very long threshold runs were essentially identical, indicating that the standard length ($n_{\mathrm{thr}} = 2.5 \times 10^5$) was sufficient to sample the possible transitions within a pocket.

However, the major result was the fact that for a given $x_i^{(h)}$ the quench runs nearly always only ended in one and the same local minimum. In 26 out of the above 31 instances, all quenches reached the same minimum, and in four cases 90% of the quenches reached the same minimum, indicating that these points belonged to the rim of the respective minima. Only one halting point clearly belonged to a transition region, with the outcome of the quench runs evenly distributed over two local minima. This is particularly noteworthy, since the energies of all the halting points were significantly above those of the saddle points within the respective pockets.

This result suggests the hypothesis that a large part of the configuration space can be associated with particular local minima, in the sense that the probability of reaching this one minimum via a stochastic quench is very large, even though in principle many local minima are accessible, if we only consider the energies of the lowest barriers among them. Conversely, the saddle regions between such 'basins' appear to be rather narrow.

This result was confirmed by an extended analysis of the pocket containing the minima VI-a and VII-a using very long threshold runs (5×10^6 steps) with 25 independent quench runs for each halting point ($n_{\mathrm{h}} = 5 \times 10^4$, or $n_{\mathrm{h}} = 5 \times 10^5$; $L_k = -6.1, -6.0, -5.9, -5.8$ eV/atom). It was found that for each halting point all the quench runs ended in the same minimum (either

[4] If such regions are locally ergodic, one can treat Q as an order parameter, and use the density of states in the region $g(E; Q)$ to calculate the local free energy $F(Q)$, with all the statistical mechanical implications.

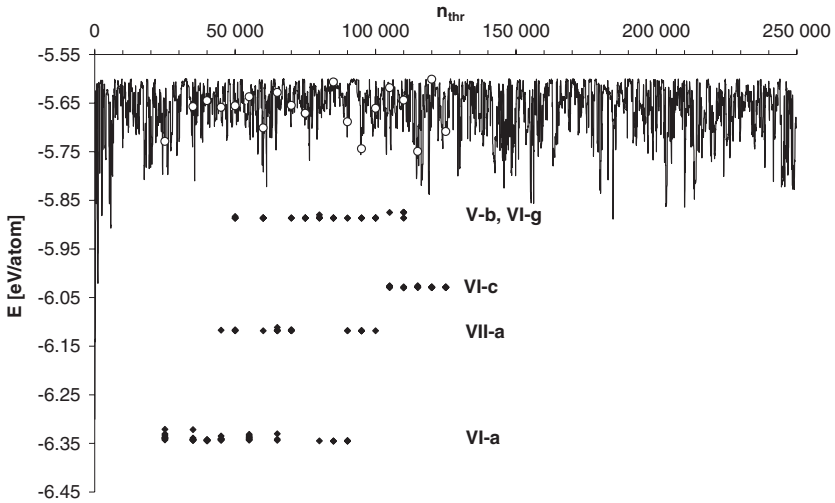

Figure 2. Transition VI-a to VI-c. Energy curve of the threshold run with halting points (white circles) between $n_{\mathrm{thr}} = 2.5 \times 10^4$ and $n_{\mathrm{thr}} = 1.25 \times 10^5$. Black diamonds show the energies of the end configurations of quench runs.

VI-a or VII-a, respectively). Thus it appears that we would need a much higher resolution, i.e. higher density of halting points, in order to find a sizeable number of points belonging to transition regions[5].

3.2. Detailed analysis of transition paths

The global (with respect to the pockets chosen) investigations in the preceding subsection suggest that the saddle regions are quite small compared to the minimum regions. In order to obtain a better estimate of the actual size of the transition regions, three complete random walks where transitions between deep-lying local minima in the system MgF_2 had occurred during threshold runs were investigated in detail. The three runs chosen were VI-a $\rightarrow$ VII-a ($L_k = -5.8, n_{\mathrm{thr}} = 5 \times 10^4, n_{\mathrm{h}} = 10^3$), VII-a $\rightarrow$ VI-a ($L_k = -6.1, n_{\mathrm{thr}} = 5 \times 10^4, n_{\mathrm{h}} = 10^3$) and VI-a $\rightarrow$ VI-c ($L_k = -5.6, n_{\mathrm{thr}} = 2.5 \times 10^5, n_{\mathrm{h}} = 5 \times 10^3$), where in the transition region every n_{h} steps ten long quench runs were performed. In order to convey an impression of the energy profiles of these runs, an excerpt from the run VI-a $\rightarrow$ VI-c is depicted in figure 2. Profiles for the other runs can be found in [41]. The $x_i^{(h)}$ are indicated by white circles, and the energies of the final configurations of the quench runs are shown as black diamonds.

3.2.1. MgF_2: VI-a $\rightarrow$ VII-a. Along the path, the system was found about 6% of the time in the transition region, and the transition itself took place in a narrow range $n_{\mathrm{thr}} = 3.5 \times 10^4$–$3.7 \times 10^4$, giving an estimated width of $\approx 3 \times 10^3$ MC steps for the transition region. Only once, a high-lying side-minimum corresponding to a prism structure (VI-g) was found.

For halting points outside the transition range, the topology of the structures $x_i^{(h)}$ usually resembled the minimum reached after the quench run, m_A (VI-a or VII-a), sufficiently to allow a visual identification, although $E(x_i^{(h)})$ was considerably higher than $E(m_A)$ and the energy of the saddle between VI-a and VII-a.

[5] Of course, since we are using a stochastic quench algorithm, it is not possible to define precise widths of the transition regions—all statements will be subject to statistical errors.

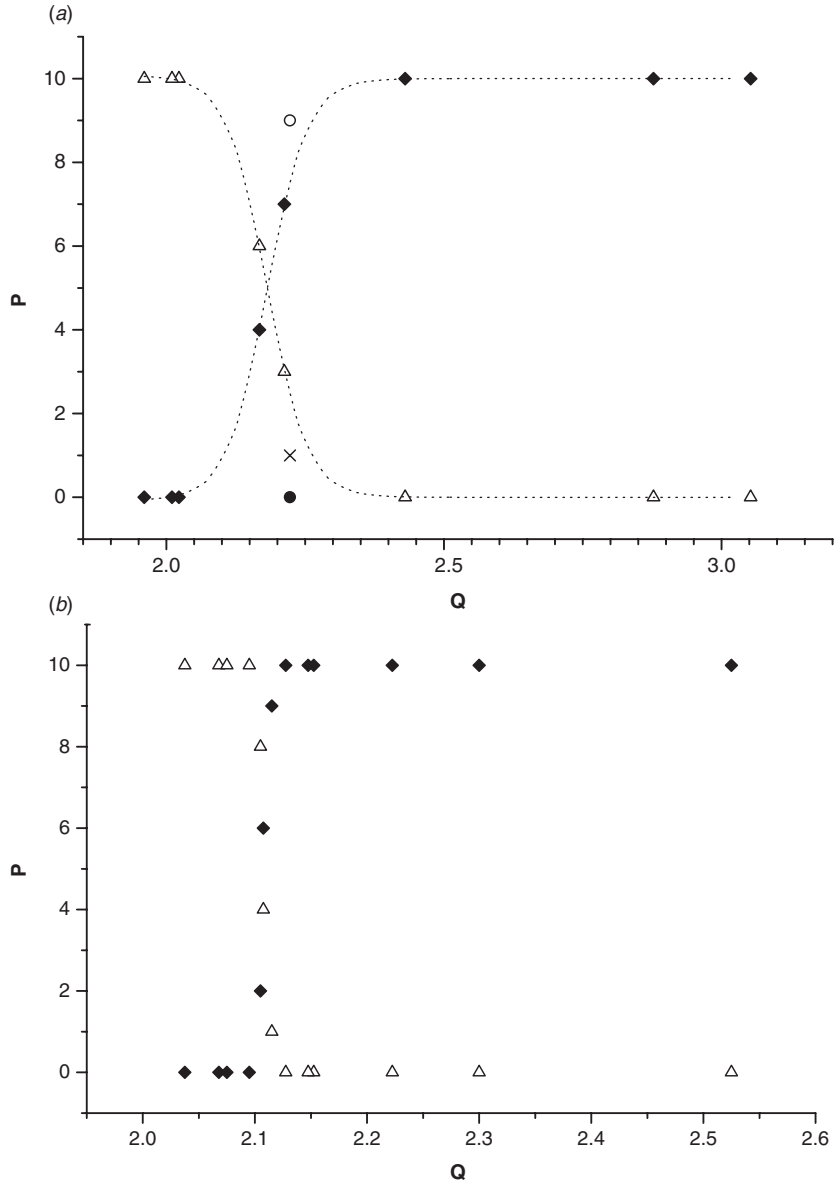

Figure 3. Probabilities $P(m_A)$ of reaching various local minima m_A versus structure coordinate Q(VI-a, VII-a) for the halting points along the threshold trajectory VI-a–VII-a in the energy range around -5.6 eV/atom (a) and along the threshold trajectory VII-a–VI-a in the range around -6.0 eV/atom (b). Ten quench runs were performed at each halting point. Black diamonds, P(VI-a); white triangles, P(VII-a). Due to the lower energies of the halting points, the range of the Q-values is smaller in (b) than in (a). The points at $Q = 2.22$ belong to a different part of the energy landscape (see text); here, black circle, P(VI-a); $\times$, P(VI-g); white circle, P(VII-a). The values of Q for the actual minima VII-a and VI-a are 2.04 and 2.76, respectively. The dotted curves are drawn as a guide to the eye.

In figure 3(a), the quench probabilities $P(Q)$ as a function of a structure parameter Q are shown. Here Q is defined as the sum of four characteristic Mg–F nearest-neighbour distances

belonging to atoms connected via the 2_1-symmetry element in the ideal VII-a structure. The values of Q for the actual minima VII-a and VI-a are 2.04 and 2.76, respectively. Two aspects of the figure should be noted: first, the quench probabilities follow a steep sigmoid, indicating that as a function of Q the transition is quite narrow, although we are at energies far above the saddle point. Furthermore, we note one point on the plot (marked by a circle), which does not fit on the curve at all. A detailed look at its probability distribution discloses that this halting point actually belongs to the transition region between VII-a and VI-g, and not to the one between VII-a and VI-a. Clearly, it is not allowable to include this point in the 'average' $P(Q)$; thus we are dealing with an example where the points x_Q belong to two different characteristic regions for the same value of Q.

3.2.2. MgF_2: VI-a → VI-c. It is no surprise that the situation is more complex along this transition path, since the energy lid is high enough to enable access to several major minima including numerous very small side minima. Figure 2 shows that the threshold random walk has actually passed through two minimum regions (VII-a at $n_h \approx 5 \times 10^4$ and V-b at $n_h \approx 10^5$) on its way to VI-c (for $n_h > 1.5 \times 10^5$). The distribution over minima found during the quench runs shows five minima as possible end configurations. In addition to those mentioned above, VI-g also was accessible from one transition region. However, it was never the sole end configuration for a set of quench runs; and thus no extended region of configuration space could be associated with it. Since too many local minima are involved along this path, it was not possible to define a simple structure parameter or set of structure parameters, and no plot $P(Q)$ is given for this example.

Analysing the geometry of the configurations showed that those $x_i^{(h)}$ that are associated with VI-a again exhibit the rutile structure, but with larger distortions due to the higher energy $E(x_i^{(h)})$ compared with the configurations in the previous section 3.2.1. After $n_h \approx 1.25 \times 10^5$, the $x_i^{(h)}$ essentially resemble the VI-c minimum, while in between $x_i^{(h)}$ show mostly the characteristics of the V-b minimum. Overall, along this path, the system is found in transition regions about 15% of the time. The widths of the various transition regions explored during this random walk were about one order of magnitude larger than for the VII-a/VI-a transition region at lower energies ($\approx 10^4 - 2 \times 10^4$ MC steps).

3.2.3. MgF_2: VII-a → VI-a. Along the path, the system was found about 2% of the time in the transition region, whose width in MC steps is estimated to be about $\approx 2 \times 10^3$, which is comparable to that observed in section 3.2.1.

The analysis of the geometric structures of the configurations x_i^h for $n_h = 1 \times 10^4$–2×10^4 shows that up to $n_h = 1.7 \times 10^4$ the sevenfold coordination (Mg by F) of the VII-a-structure and the corresponding connections among atoms are approximately preserved. The sixfold coordination (Mg by F) and the general topology of rutile (i.e. rows of edge-connected polyhedra linked by opposite vertices to the next rows) is reached for $n_h > 1.8 \times 10^4$. At first sight, this suggests that the transition takes place around $n_h = 1.7 \times 10^4$, supported by the fact that the energy profile always remains above E(VII-a) for $n_h < 1.8 \times 10^4$. However, the transition range is actually reached much earlier during the threshold run, since for halting points between $n_h = 9 \times 10^3$ and $n_h = 1.7 \times 10^4$ the quench runs exclusively end up in the minimum VI-a. Although the starting configurations still exhibit the features of the sevenfold coordination, one crucial pair of distances between Mg and F is already characteristically elongated (cf the definition of Q in section 3.2.1), thus initiating the transformation into a sixfold coordination.

In figure 3(*b*), we show again $P(Q)$, using the same definition for Q as in section 3.2.1.

The shape of $P(Q)$ is again a sigmoid, but since we are dealing with a lower energy slice ($L = -6.1$ eV/atom versus $L = -5.8$ eV/atom in section 3.2.1) the transition between VI-a and VII-a is even narrower, and the range of observed Q-values is somewhat smaller.

4. Discussion and outlook

The analysis of the halting points, both for the global exploration and along the transition paths, in the preceding section can be summarized as follows: the actual saddle regions, where there is a high probability (>10%) for a quench run to reach different local minima, are quite small: even along paths that connect two or more minimum regions, the width of the transition regions is only on the order of a few 10^3 to a few 10^4 MC steps, with the larger value found for random walks at higher energies. The time within the transition regions has to be contrasted with the time spent within the minimum regions, which is about one order of magnitude larger. This correlates nicely with the results of the global explorations, which also suggest that the size of the minimum regions is considerably larger than the transition regions.

A second closely related result of this analysis is that many states with energies high above the energy barriers still can be assigned unambiguously to certain local minima based on the criterion of the end configurations of stochastic quench runs. This is strongly supported by the observation that, geometrically and topologically, these high-lying states bear a strong resemblance to the accessible minima in the pocket.

Of course, the sample size for random walks on the energy landscape is not large enough for a complete coarse-grained description of the landscape. Nevertheless, the runs presented in the previous section allow us to construct a first qualitative model of the explored portion of the VI-a–VII-a pocket[6] from the observed characteristic regions (cf figure 4). One notices that this representation of the pocket is not a tree model but a graph containing circuits. In addition, we see that even at high energies the minimum regions are much larger than the transition regions, although we have focused on random walks that visit at least two minima. Finally, we note that at higher energies saddles connecting several minima make up a sizeable fraction of the transition regions.

Even without a detailed analysis of the system's dynamics on the characteristic regions graph, the relative sizes of minimum (S_M) and transition (S_T) regions can already serve as a first indication of the chemical system's tendency to form crystalline ($S_M \gg S_T$) and amorphous ($S_T \gg S_M$) compounds, respectively. Furthermore, the sizes of minimum regions at moderate to high energies are an indication of the thermal stability of the compound corresponding to the particular minimum[7]. For example, for our model system, the results would suggest that MgF_2 should form stable crystalline compounds (at least up to moderate temperatures).

Similarly, the range of minima accessible from points within the transition regions as a function of temperature can yield information about possible phase transitions. Such an analysis has been performed for amorphous $Si_3B_3N_7$ [42]. Here, the distributions of local minima that could be reached by quench runs from halting points $x_i^{(h)}$ along long MC trajectories were investigated for a large range of temperatures. For each set of minima $\{m(x_i^{(h)})\}$, the mean rms distance among these minima was computed, and the average over all these mean values was calculated for each temperature. This average minimum–minimum

[6] In this paper, we did not include the transitions to the minima VI-d, VI-e and V-a, which are also accessible, in principle, for $L_k = -5.6$ eV/atom (cf figure 1). However, these minima are considerably more remote from the centre of the pocket than for example VI-c, as one can see from the transition maps for the system in [33]—an example where the tree graph taken by itself can give a misleading impression.

[7] Clearly, such information about the sizes of characteristic regions can also be useful for the design of efficient global optimization strategies on multi-minimum cost function landscapes.

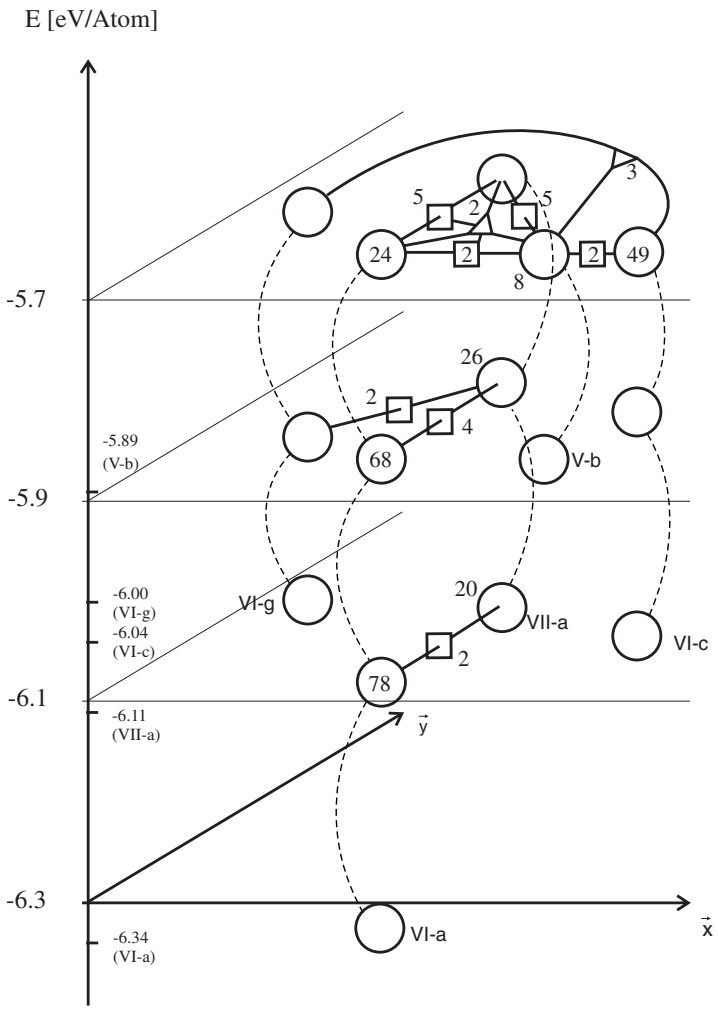

Figure 4. Graph representation based on characteristic regions derived from threshold runs with different lids for the pocket of the energy landscape of MgF_2 containing the major minima VI-a, VII-a and VI-c. Energies of the minima involved are given in eV/atom. Circles indicate accessible local minima; squares and triangles represent saddles connecting two and three minima, respectively. For each energy level, the percentage of the random walks spent in a characteristic region is listed next to the symbol (circles without percentages indicate those regions that were only visited during the quench phase and not during the statistically relevant threshold phase). Solid curves connect those characteristic regions within one energy range that are neighbours according to the random walks. Dashed curves connect the minimum characteristic regions between different energy levels.

distance increased monotonically with temperature, with a sharp increase by about an order of magnitude at a temperature T_F that corresponded to the 'freezing' temperature of the system.

In this context, it would be very interesting to compare and possibly combine the characteristic regions presented here with the so-called inherent structures on landscapes of disordered systems [43], which are obtained by using a deterministic (gradient-based) technique for local optimization. In the latter case the focus is on the fastest downhill path ignoring other routes of descent available, and $x^{(h)}$ is uniquely assigned to some critical point

of the landscape (minimum, saddle) resulting in a sharp division of the landscape. In contrast, the stochastic quench runs produce a probability distribution over the local minima that are accessible from $x^{(h)}$, $W(x^{(h)})$, which changes only gradually as function of $x^{(h)}$. Thus, the true size of a saddle region and the range of accessible minima can be perceived when employing the stochastic approach—quantities that are expected to be closely connected to the relaxation behaviour of realistic systems at finite temperatures.

While the methodology presented in this paper is applicable to all multi-minimum energy landscapes, the current computational limitations make the comparison between experiment and theory rather difficult[8]. However, study of more and more 'realistic' systems is clearly going to be needed, if one wants to reach the point where a valid comparison with experiment becomes feasible.

Here, the characteristic region analysis can provide us with a general procedure to go beyond the tree-graph models when constructing simplified representations of landscapes. Already the more easily obtainable information about the relative sizes of transition and minimum regions should serve as valuable input to abstract tree models of landscapes. However, this approach towards increasingly realistic models will have to be complemented by the investigation of simplified model systems, where one has more control about the relation between energy and relative positions of the states in configuration space, if one wants to reach a deeper understanding of the properties of energy landscapes.

Acknowledgments

We would like to thank Z Çançareviç for assistance with figure 4. CS acknowledges fruitful discussions at workshops on energy landscapes at the Telluride Summer Research Center in 1997 and 1999. This work was partly funded by the DFG via SFB408.

Appendix

In earlier work [30], we have shown how one can derive bounds on the energy barriers between the minima, and estimates of the local densities of states from the combined outcome of such threshold runs. In order to estimate the length n_{thr} of the threshold runs needed to sample the pocket, we compare the sampling of the local density of states for one of the minima employed in this paper, VI-a (rutile) in the MgF_2 system, for six different lid levels $L_{1-6} = -5.8, -5.7, -5.6, -5.5, -5.4, -5.0$ eV/atom. We observe that the major features of the local density of states are already accessible for $n_{\mathrm{thr}} = 5 \times 10^4$ (cf figure 3.1 in [41]).

In contrast, the occurrence of transitions is expected to be influenced more strongly by the length of the threshold phase, but while doubling n_{thr} from 2.5×10^5 to 5×10^5 leads in some rare instances to a slight reduction in the lowest lid values where the transition is present, the basic structure of the tree graphs does not change. Only for very short runs ($n_{\mathrm{thr}} = 10^4$) do we observe major rearrangements of the trees. Thus, we chose $n_{\mathrm{thr}} = 2.5 \times 10^5$ as the standard length for the threshold runs. As a further check, we repeated these test runs for many different random numbers, starting from VI-a. The general properties of the transitions were preserved: the energy barriers to other important local minima in the pocket (e.g. VI-c and VII-a) did not change and the percentage of transitions into these minima remained essentially the same.

[8] The work presented took the equivalent of about 2 years computing on a single high-end work station.

References

[1] Frauenfelder H, Bishop A R, Garcia A, Perelson A, Schuster P, Sherrington D and Swart P J (ed) 1996 *Physica* D **107** nos 2–4, special issue *Landscape Paradigms in Physics and Biology*
[2] Palmer R 1982 *Adv. Phys.* **31** 669
[3] Schön J C and Jansen M 2001 *Z. Krist.* at press
[4] Götze W and Sjögren J 1992 *Rep. Prog. Phys.* **55** 241
[5] Jäckle J 1986 *Rep. Prog. Phys.* **49** 171
[6] Ramakrishnan T V and Lakshmi M R (ed) 1987 *Non-Debye Relaxation in Condensed Matter* (Singapore: World Scientific)
[7] Dasgupta C and Valls O T 1998 *Phys. Rev.* E **58** 801
[8] Schön J C and Paolo Sibani 1998 *J. Phys. A: Math. Gen.* **31** 8167
[9] Fischer K H and Hertz J A 1991 *Spin Glasses* (Cambridge: Cambridge University Press)
[10] Sibani P 1998 *Physica* A **258** 249
[11] Bryngelson J D, Onuchic J N, Socci N D and Wolynes P G 1995 *Prot. Struct. Funct. Gen.* **21** 167
[12] Dill K A, Bromberg S, Yue K, Fiebig K M, Yee D P, Thomas P D and Chan H S 1995 *Prot. Sci.* **4** 561
[13] Onuchic J N, Luther-Schulten Z and Wolynes P G 1997 *Annu. Rev. Phys. Chem.* **48** 539
[14] Dobson C M, Sali A and Karplus M 1998 *Angew. Chem. Int. Edn Engl.* **37** 868
[15] Berry R S 1993 *Chem. Rev.* **93** 2379
[16] Becker O M and Karplus M 1997 *J. Chem. Phys.* **106** 1495
[17] Schön J C and Jansen M 1996 *Angew. Chem. Int. Edn* **35** 1286
[18] Schön J C and Jansen M 1999 *Pauling's Legacy: Modern Modeling of the Chemical Bond* ed Z Maksic and W Orville-Thomas (Amsterdam: Elsevier) p 103
[19] Sibani P, Schön J C, Salamon P and Andersson J-O 1993 *Europhys. Lett.* **22** 479
[20] Schön J C 1997 *J. Phys. A: Math. Gen.* **30** 2367
[21] Berry R S and Breitengraser-Kunz R 1995 *Phys. Rev. Lett.* **74** 3951
[22] Davis H L, Wales D J and Berry R S 1990 *J. Chem. Phys.* **92** 4308
[23] Nichols J, Taylor H, Schmidt P and Simons J 1990 *J. Chem. Phys.* **92** 342
[24] Sun J-Q and Ruedenberg K 1994 *J. Chem. Phys.* **101** 2157
[25] Cerjan C J and Miller W H 1981 *J. Chem. Phys.* **75** 2800
[26] Quapp W 1996 *Chem. Phys. Lett.* **253** 286
[27] Daldoss G, Pilla O, Viliani G and Brangian C 1999 *Phys. Rev.* B **60** 3200
[28] Berry R S 1994 *J. Chem. Phys.* **98** 6910
[29] Hoffmann K H and Sibani P 1988 *Phys. Rev.* A **38** 4261
[30] Schön J C 1996 *Ber. Bunsenges.* **100** 1388
[31] Wales D J, Miller M A and Walsh T R 1998 *Nature* **394** 758
[32] Heuer A 1997 *Phys. Rev. Lett.* **78** 4051
[33] Wevers M A C, Schön J C and Jansen M 1999 *J. Phys.: Condens. Matter* **11** 6487
[34] Schön J C, Putz H and Jansen M 1996 *J. Phys.: Condens. Matter* **8** 143
[35] Wevers M A C, Schön J C and Jansen M 1998 *J. Solid State Chem.* **136** 223
[36] Metropolis N, Rosenbluth A W, Rosenbluth M N, Teller A H and Teller E 1953 *J. Chem. Phys.* **21** 1087
[37] Klotz T and Kobe S 1994 *Acta Phys. Slov.* **44** 347
[38] Klotz T, Schubert S and Hoffmann K H 1998 *J. Phys.: Condens. Matter* **10** 6127
[39] Uhlig C, Hoffmann K H and Sibani P 1995 *Z. Phys.* B **96** 409
[40] Hoffmann K H, Schubert S and Sibani P 1997 *Europhys. Lett.* **38** 613
[41] Wevers M A C 2000 *PhD Thesis* University of Bonn
[42] Hannemann A, Schön J C and Jansen M 2001 in preparation
[43] Stillinger F H 1995 *Science* **267** 1935